ARCHIVES
of
FOUNDRY ENGINEERING

ISSN (2299-2944)
Volume 2025
Issue 3/2025

189 – 194

10.24425/afe.2025.153797

21/3

Published quarterly as the organ of the Foundry Commission of the Polish Academy of Sciences

Effect of Fe Amount on Microstructure and Fluidity of A356 Alloy

M. Durmus [a], D. Dispinar [b,*], M. Gavgali [a], M. Colak [c]
[a] Necmettin Erbakan University, Turkey
[b] SINTEF Industri, Metal Production and Processing, Trondheim, 7034, Norway
[c] Bayburt University, Turkey
* Corresponding author: e-mail: derya.dispinar@gmail.com

Received 14.10.24; accepted in revised form 30.01.25; available online 26.08.2025

Abstract

The most important factor affecting the production of quality parts with aluminum alloys is the quality of molten metal. One of the determining factors in molten metal quality is the minimization of trace impurity elements in the alloy. One of the most harmful impurities among these elements is Fe, and its amount is a determining factor in its negative effect. It is known that Fe negatively affects the quality of aluminum, causing a decrease in mechanical properties. Most of the Fe in the alloy forms intermetallic from needle-like to complex Chinese-script structures. In this study, carbon steel and stainless-steel rods were immersed in the liquid metal at casting temperatures of 700°C and 750°C in A356 aluminum casting alloy and were subjected to diffusion for 1, 2 and 5 hours. Subsequently, a 4-channel flow test mold with various section thicknesses was used. All samples were measured by measuring the liquid metal advance distances of all sections in mm. Then, microstructure analyses were performed on the obtained sections. As a result, it is observed that as Fe diffusion increases, liquid metal advancement distances decrease and Fe intermetallics form in the microstructure.

Keywords: A356, Fe content, Intermetallic, Fluidity, Fluidity index

1. Introduction

Aluminum alloys are widely used in many applications such as automotive and aerospace due to their low density, excellent mechanical properties, light weight, easy fabrication, strength and good corrosion resistance [1-4]. The quality of the final product needs to be high due to critical application areas. It is well-known that the factors affecting the casting quality of aluminum casting alloys are alloy composition, casting temperature, microstructure, and porosity. Various factors occurring in the structure can cause microporosity, oxide film and intermetallic phases that affect the mechanical properties of the alloy [5-9].

The microstructure of aluminum casting alloys plays an important role in determining their mechanical properties and overall quality. Optimizing the casting temperatures in aluminum alloys is a critical factor to improve the quality and performance of the final product. [10]. Studies have shown that factors such as cooling rates during the casting process can affect the microstructure, with slower cooling rates leading to coarse dendritic morphology and adverse effects on the strength and elongation of the cast parts [11,12]. Many elements in the alloy have different characteristics on the microstructure. One of these elements, iron, which is either intentionally or unintentionally present in the alloy, has a complex effect on the casting quality of aluminum alloys. Fe is considered to be the most widespread and harmful impurity in aluminum casting alloys, causing an increase in casting defects that can adversely affect the properties of the material [13-15]. The presence of Fe can promote the formation of intermediate phases in the solidification process of aluminum alloys [16-20]. While Fe forms an intermetallic, its morphology varies depending on the other alloying elements present in the

liquid metal. Particularly, Si, Mn and Cr content have major control over the size and shape of Fe-based intermetallic phases in which it can be in the form of needle (beta Fe) or Chinese script (alpha Fe) morphologies.

Fluidity in aluminum alloys is a critical property affected by various factors. Factors such as Fe, intermetallics, structural properties of the surface film layer, presence and distribution of defects in aluminum alloys are among these factors [21,22]. The fluidity of aluminum alloys can vary depending on factors such as the amount of Fe they contain, the composition of the alloy, and the solidification process. Therefore, in order to understand the effect of the Fe element on fluidity in aluminum alloys, various factors such as solidification rate, microstructure, and mechanical properties must be evaluated together. The presence of iron in aluminum alloys can affect their fluidity by promoting the formation of intermediate phases during solidification.

In this study, A356 alloy, carbon steel and stainless-steel rods were diffusion immersed in liquid metal at 700°C and 750°C for 1, 2 and 5 hours. Then, they were cast in a 4-channel fluidity mold with different section thicknesses.

2. Experimental work

The chemical composition of the A356 aluminum alloy is given in Table 1. The chemical compositions of the steel bars used to examine the effect of diffusion and changes in the microstructure are given in Table 2.

Table 1.
A356 Aluminum Alloy Chemical Composition (%wt)

Fe	Si	Cu	Mn	Mg	Zn	Ni	Ti	Al
0,20	6,65	0.02	0.03	0,33	0.04	0,02	0,08	Rem.

Table 2.
Chemical Composition of Steel Bars (%wt)

	C	Mn	P	S	Si	Cr	Ni
SS430	0,12	1,0	0,045	0,03	1,0	16	0,75
St1020	0.18	0.4	0,04	0,05	-	-	-

In the experimental setup, two different casting temperature (700 °C-750 °C), two different steel rods (carbon steel - stainless steel), and three different holding times (1 hour, 2 hours and 5 hours). Overall, 14 different castings were made. Castings were carried out in a SiC crucible in the induction furnace as shown in Figure 1. When the liquid metal temperature reached the desired value, carbon and stainless steel rods with a diameter of 40 mm were kept in the liquid metal.

Fig. 1. Visual of steel rod in induction furnace and crucible used in casting

Castings were made in a permanent mold. The mold was heated to approximately 250 °C with a heating table. Then, samples were collected for microstructural analysis. Castings were made in a permanent mold and samples were collected for microstructural analysis. After polishing, the samples were etched with Keller's solution (95 ml distilled water, 2.5 ml HNO3, 1.5 ml HCl, 1.0 ml HF). After etching, the microstructure was examined using an NMM-800/820 series metallurgical optical microscope. Additionally, fluidity tests were performed on 4-channel permanent mold castings with thicknesses ranging from 2 to 8 mm (Figure 2).

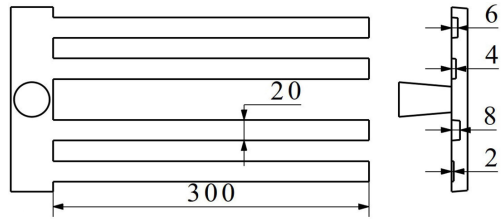

Fig. 2. Dimension of the fludity mould

3. Results and Discussion

An example sample image obtained from castings is given in Figure 3.

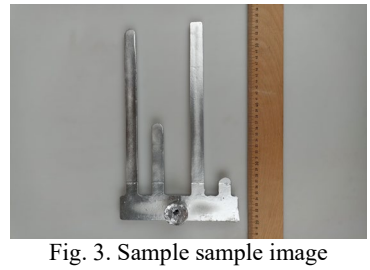

Fig. 3. Sample sample image

In the study, the chemical analysis results of the cast samples under varying conditions given in experimental section are provided in Table 3. The tests were analyzed with the ARL brand optical spectrometer and EN 1706 standard. When the results obtained from OES analysis are examined, it can be seen that the casting temperature and diffusion time are the most effective parameters in the change of Fe content in the melt. Additionally, the increase in Ni and Cr content was also reported mainly due to the dipping of stainless-steel rods. It is important to note that Si content starts to decrease in longer durations that is attributed to increased formation of AlFeSi phases in which they start to sedimate to the bottom of the crucible.

Table 3.
Chemical analysis results of the test samples (% wt.)

Material	exp	Si	Fe	Mn	Ni	Cr
None	700-D0	7,140	0,108	0,002	0,003	0,001
	750-D0	7,011	0,112	0,002	0,005	0,007
Carbon Steel	700-D1	7,171	0,121	0,008	0,003	0,001
	700-D2	7,241	0,310	0,003	0,004	0,001
	700-D5	5,861	1,973	0,017	0,003	0,003
	750-D1	5,784	1,450	0,009	0,011	0,003
	750-D2	5,795	1,985	0,109	0,007	0,003
	750-D5	5,294	2,359	0,013	0,008	0,003
Stainless Steel	700-D1	7,014	0,458	0,009	0,024	0,033
	700-D2	6,360	1,100	0,027	0,049	0,056
	700-D5	6,610	1,390	0,037	0,091	0,134
	750-D1	6,540	1,220	0,036	0,090	0,119
	750-D2	6,559	1,670	0,045	0,134	0,263
	750-D5	6,453	1,709	0,047	0,144	0,281

When the images given in Figure 4 are examined, it is seen that when the casting temperature is changed, no Fe-based intermetallic phases observed considering the 0.1 wt% Fe content of the base alloy. The pictures of the specimens obtained from carbon steel diffusion castings are given in Figure 4.

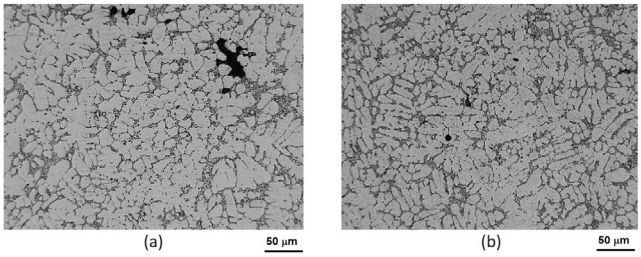

Fig. 4. Microstructure images of reference samples
(a) 700ºC, (b) 750ºC

When carbon steel was dipped for 1, 2 and 5 hours; it is seen in Figure 5 that the intermetallic formation starts, and the pore sizes are smaller at 700°C at 1 hour diffusion time. When the diffusion time is 2 hours, it is seen that the pore size and number increase and intermetallic formation is also increased. When the diffusion time was 5 hours, it was observed that the β phase, known as the most harmful phase, increased significantly with localized distribution. Also, the pore formation was increased with pores particularly accumulated around the Fe phases. When the diffusion temperature was increased from 700°C to 750°C, the intermetallic phase formation, pore distribution and their sizes were increased dramatically with increased the diffusion time. It is important to note that there was a significant increase in the length and width of the β phase at diffusion times of 2 and 5 hours. When the temperature difference is examined, it is seen that the number and size of phases formed at 700°C 1, 2 and 5 hours are less than 750°C. This is due to the fact that the temperature increases the diffusion rate.

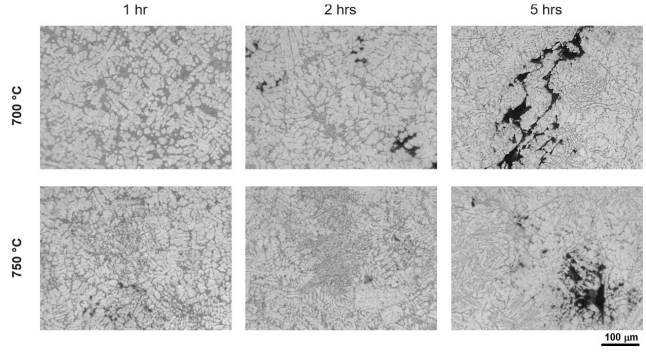

Fig. 5. 100X microstructure images of samples exposed to diffusion with plain carbon steel

When the microstructures given in Figure 6 are examined, the size and distribution of the pores and Fe intermetallic phases were directly related with the diffusion time. The different type and morphology of Fe phases were recorded in the microstructure. One of the reasons for this is the increase in Cr and Ni content as well as the increase in the Fe content in the chemical composition. Considering the diffusion hours and temperatures applied to the liquid metal, less and smaller phases was formed in 1 hour at 700°C. When the diffusion time is 2 and 5 hours, it is observed that β-Al5FeSi (needle structure), α phase (writing-like) formation and pore formation increase. When the diffusion effect for 1, 2 and 5 hours at 750°C was examined, it was observed that as the diffusion time increased, there was an increase in the intermetallic, and also porosity formed in the structure. When the effect of casting temperature is examined, it is seen that less intermetallic is formed at 700°C when compared to 700°C and 750°C. It is thought that this is due to the fact that temperature increases the diffusion rate.

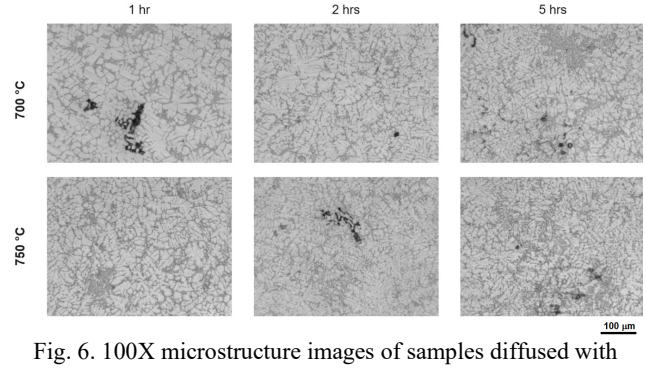

Fig. 6. 100X microstructure images of samples diffused with stainless steel

In Figure 7, a representative image of a sample where carbon steel was dipped is given. It can be clearly seen that the microstructure is consisted of β-AlFeSi phases. In Figure 8, when stainless steel was used, Cr, Ni and Mn were detected in the EDX analysis.

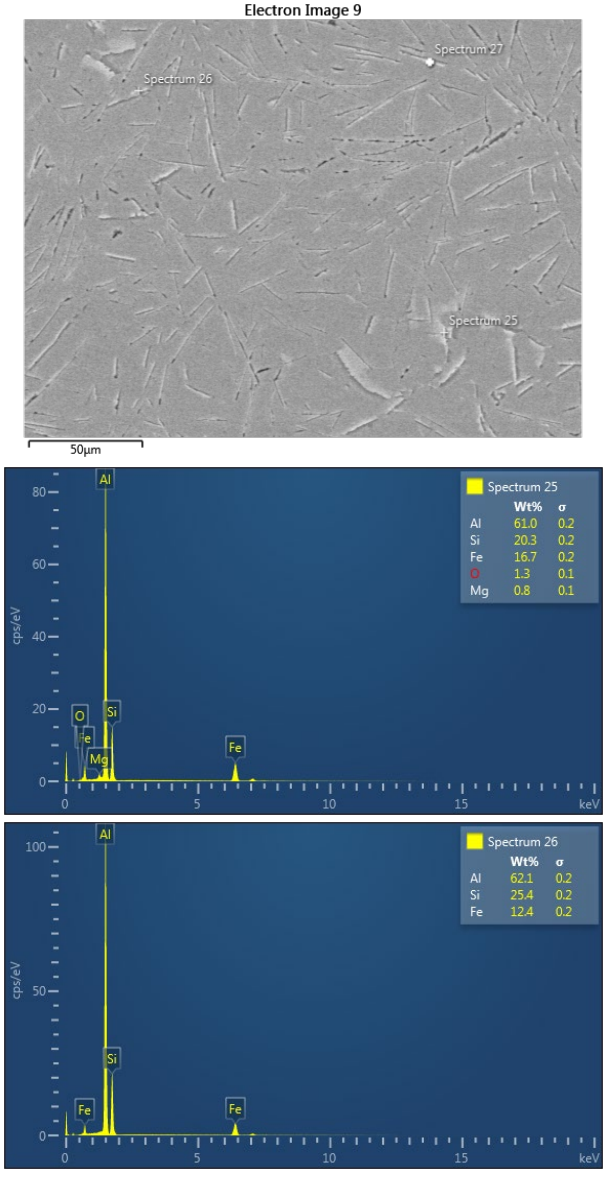

Fig. 7. SEM and EDX analysis of samples with carbon steel

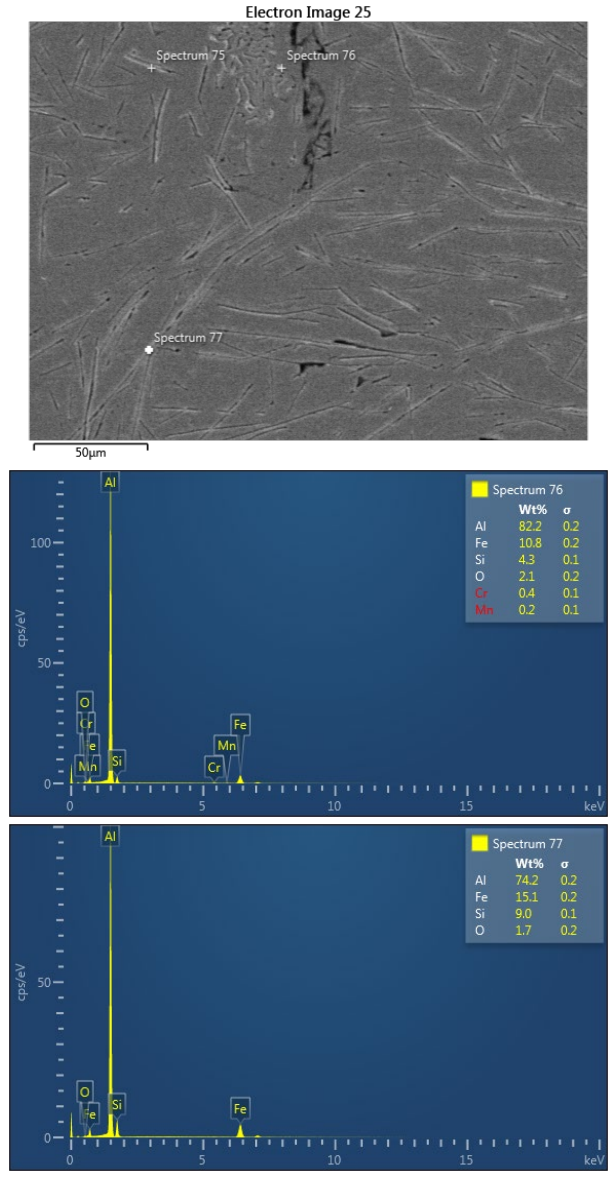

Fig. 8. SEM and EDX analysis of samples with stainless steel

The values obtained from the four-channel fluidity pattern are given in the fluidity index formula given below and the fluency index values obtained in Table 4. When calculating the fluidity index, it can be calculated by expanding it depending on the number of channels in the mold where this index is located [21].

$$Fluidity\ index = \frac{Liquid\ Metal\ Advancement\ Distance\ (mm)}{Section\ Thickness\ (mm)}$$

Calculations for the fluidity mold used in the experiments were made as in the example below. The sample calculation was carried out with the liquid metal advance distances obtained in the 700°C reference casting.

$$Fluidity\ index = \frac{4}{2} + \frac{144}{4} + \frac{217}{6} + \frac{300}{8} = 111{,}67$$

Table 4.
Fluidity index values of the samples

Material	Time	700°C	750°C
None		111,6	126,1
Carbon Steel	1	48,8	82,0
	2	36,7	56,6
	5	35,4	49,5
Stainless Steel	1	51,0	73,0
	2	38,0	59,4
	5	28,2	36,8

The fluidity test results are summarized in Figure 9. It can be seen that the fluidity increases with increased casting temperature, and it decreases with increased Fe content of the alloy. When the fluidity difference between carbon steel and stainless-steel dipped samples are compared, it could be seen that there is no significant difference in the fluidity lengths at different section thicknesses.

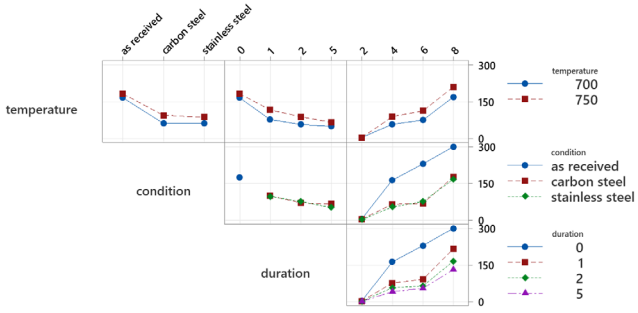

Fig. 9. Fluidity index change of A356 alloy at different casting temperature and section thickness

4. Conclusions

The results obtained from the studies are given below.

- After dipping steel rod in liquid aluminum, increasing the casting temperature from 700°C to 750°C, Fe content was increased due to the increase in the diffusion rate.
- When stainless steel was dipped into the alloy, an increase in Cr and Ni content as well as an increase in Fe content was recorded.
- The dipping of carbon steel and stainless steel in melts at 750°C increased the intermetallic phases as well as porosity in the microstructure.
- Microstructure examinations showed that increasing the diffusion time from 1 hour to 5 hours increased the formation of intermetallic and pores in the alloy.
- Beta-Fe phase size and distribution was increased with increased temperature and duration.
- In the presence of Cr and Ni, more complex Fe-phases together with switch from beta to alpha Fe formation was observed.
- Less pores were observed in stainless steel dipped melts compared to carbon steel dipped melts.
- Both the fluidity and the fluidity index were decreased with increasing Fe content.
- Increasing the casting temperature increases the fluidity index
- Fluidity index is decreased higher when stainless steel was used compared to carbon steel.

Conflict of interest

On behalf of all authors, the corresponding author states that there is no conflict of interest.

References

[1] Stojanović, B., Bukvic, M. & Epler, I. (2018). Application of aluminum and aluminum alloys in engineering. *Applied Engineering Letters Journal of Engineering and Applied Sciences.* 3(2), 52-62. https://doi.org/10.18485/aeletters.2018.3.2.2 .

[2] Kadhim, M.H., Latif, N.A., Harimon, M.A., Shamran, A.A. & Abbas, D.R. (2020). Effects of side-groove and loading rate on the fracture properties of aluminium alloy AL-6061. *Materialwissenschaft und Werkstofftechnik*. 51(6), 758-765. https://doi.org/10.1002/mawe.201900262.

[3] Pantelakis, S., Setsika, D., Chamos, A. & Zervaki, A. (2016). Corrosion damage evolution of the aircraft aluminum alloy 2024 T3. *International Journal of Structural Integrity*. 7(1), 25-46. https://doi.org/10.1108/IJSI-03-2014-0010.

[4] Gursoy, O., Nordmak, A., Syversten, F., Colak, M., Tur, K. & Dispinar, D. (2021). Role of metal quality and porosity formation in low pressure die casting of A356: experimental observations. *Archives of Foundry Engineering*. 21(1), 5-10. DOI: 10.24425/afe.2021.136071.

[5] Lu, G., Huang, P., Yan, Q., Xu, P., Pan, F., Zhan, H. & Chen, Y. (2020). Optimizing the microstructure and mechanical properties of vacuum counter-pressure casting ZL114A aluminum alloy via ultrasonic treatment. *Materials*. 13(19), 4232, 1-13. https://doi.org/10.3390/ma13194232.

[6] Yan, Q.S., Lu, G., Luo, G.M., Xiong, B. W. & Zheng, Q.Q. (2018). Effect of synergistic action of ultrasonic vibration and solidification pressure on tensile properties of vacuum counter-pressure casting aluminum alloy. *China Foundry*. 15, 411-417. https://doi.org/10.1007/s41230-018-8048-8.

[7] Zhang, B., Cockcroft, S.L., Maijer, D.M., Zhu, J.D. & Phillion, A.B. (2005). Casting defects in low-pressure die-cast aluminum alloy wheels. *The Journal of The Minerals, Metals & Materials Society*. 57, 36-43. https://doi.org/10.1007/s11837-005-0025-1.

[8] Chen, Y.J., Huang, L.W. & Shih, T.S. (2003). Diagnosis of oxide films by cavitation micro-jet impact. *Materials Transactions*. 44(2), 327-335. https://doi.org/10.2320/matertrans.44.327.

[9] Uslu, E., Dağ, M.M. & Çolak, M. (2023). Design and manufacturing of reduced pressure test machine for

determination of liquid aluminum quality in casting. *Turkish Journal of Electromechanics and Energy*. 8(3), 85-89.
[10] Jakse, N. & Pasturel, A. (2013). Liquid aluminum: atomic diffusion and viscosity from ab initio molecular dynamics. *Scientific reports*. 3(1), 3135. https://doi.org/10.1038/srep03135.
[11] Li, L., Li, D., Feng, J., Zhang, Y. & Kang, Y. (2020). Effect of cooling rates on the microstructure and mechanical property of La modified Al7SiMg alloys processed by gravity die casting and semi-solid die casting. *Metals*. 10(4), 549, 1-13. https://doi.org/10.3390/met10040549.
[12] Linder, J., Arvidsson, A. & Kron, J. (2006). The influence of porosity on the fatigue strength of high-pressure die cast aluminium. *Fatigue & Fracture of Engineering Materials & Structures*. 29(5), 357-363. https://doi.org/10.1111/j.1460-2695.2006.00997.x.
[13] Chen, C., Wang, J., Shu, D. & Sun, B. (2011). Removal of iron impurity from aluminum by electroslag refining. *Materials transactions*. 52(6), 1320-1323. https://doi.org/10.2320/matertrans.M2010435.
[14] Lu, L. & Dahle, A.K. (2005). Iron-rich intermetallic phases and their role in casting defect formation in hypoeutectic Al-Si alloys. *Metallurgical and materials transactions A*. 36, 819-835. https://doi.org/10.1007/s11661-005-0196-y.
[15] Saikrishnan, G., Jayakumari, L.S., Vijay, R. & Singaravelu, D.L. (2019). Influence of iron–aluminum alloy on the tribological performance of non-asbestos brake friction materials – a solution for copper replacement. *Industrial Lubrication and Tribology*. 72(1), 66-78. DOI: 10.1108/ILT-12-2018-0441.
[16] de Moraes, H.L., de Oliveira, J.R., Espinosa, D.C.R. & Tenório, J.A.S. (2006). Removal of iron from molten recycled aluminum through intermediate phase filtration. *Materials transactions*. 47(7), 1731-1736. https://doi.org/10.2320/matertrans.47.1731.
[17] Kasai, H., Morisada, Y. & Fujii, H. (2015). Dissimilar FSW of immiscible materials: steel/magnesium. *Materials Science and Engineering: A*. 624, 250-255. https://doi.org/10.1016/j.msea.2014.11.060.
[18] Zhang, L., Xiaoshu, K.A.N.G. & Zhong, B. (2020). Effects of Si content on microstructure and mechanical properties of 8079 aluminum alloy. *Research and Application of Materials Science*. 2(1). https://doi.org/10.33142/msra.v2i1.1978.
[19] Novák, P. & Nová, K. (2019). Oxidation behavior of Fe–Al, Fe–Si and Fe–Al–Si intermetallics. *Materials*. 12(11), 1748, 1-13. https://doi.org/10.3390/ma12111748.
[20] Erzi, E., Gürsoy, Ö., Yüksel, Ç., Colak, M. & Dispinar, D. (2019). Determination of acceptable quality limit for casting of A356 aluminium alloy: supplier's quality index (SQI). *Metals*. 9(9), 957, 1-14. https://doi.org/10.3390/met9090957.
[21] Zhang, G., Wang, Z., Niu, J., Xu, H. & Ren, X. (2021). Enhanced fluidity of ZL205A alloy with the combined addition of Al–Ti–C and La. *Materials*. 14(20), 6169, 1-8. https://doi.org/10.3390/ma14206169.
[22] Durmuş, M., Dispinar, D., Gavgali, M., Uslu, E. & Çolak, M. (2024). Evaluation of Fe content on the fluidity of A356 aluminum alloy by new fluidity index. *International Journal of Metalcasting*. 1-15. https://doi.org/10.1007/s40962-024-01396-4.